DOI: 10.1021/ic902091p

Inorganic Chemistry
Article

pH-Dependent Syntheses and Crystal Structures of a Series of Organic−Inorganic Hybrids Constructed from Keggin or Wells−Dawson Polyoxometalates and Silver Coordination Compounds

Hongxun Yang, Shuiying Gao, Jian Lü, Bo Xu, Jingxiang Lin, and Rong Cao*

State Key Laboratory of Structural Chemistry, Fujian Institute of Research on the Structure of Matter, Chinese Academy of Sciences, Fuzhou, 350002 Fujian, P. R. China

Received October 22, 2009

A series of silver complexes of polyoxometalates (POMs), formulated as, $[Ag_2(4,4'\text{-bpy})_2(4,4'\text{-Hbpy})(H_2O)][PW_{12}O_{40}]$ (4,4′-bpy=4,4′-bipyridine, **1**), $[Ag_4(4,4'\text{-bpy})_4][4,4'\text{-}H_2bpy][P_2W_{18}O_{62}]\cdot 4H_2O$ (**2**), $[Ag_4(4,4'\text{-bpy})_4][H_2P_2W_{18}O_{62}]\cdot 7H_2O$ (**3**), and $Na_8[Ag_3(4,4'\text{-bpy})_3][PW_{10}Ag_2O_{39}]\cdot 6H_2O$ (**4**), have been hydrothermally synthesized *in situ* at different pH. Complex **1**, based on saturated Keggin POM building blocks and silver coordination compounds, exhibits an interesting 3-fold interpenetration of diamondlike network in the POM chemistry. Different from complex **1**, complexes **2**−**3** consist of Wells−Dawson polyoxoanions and silver coordination compounds. Complex **2** represents the highest coordination number of Wells−Dawson polyoxoanions, which helps to form a high-dimensional framework with $(4\cdot 6^4\cdot 8)_4(4^4\cdot 6^{16}\cdot 8^8)$ topology. Thee-dimensional (3D) Wells−Dawson phosphotungstate **3** reveals another new topology $(4\cdot 6^4\cdot 7)(4\cdot 6^4\cdot 8)_2(4^3\cdot 6^8\cdot 7^2\cdot 8^2)$. Complex **4** forms a 3D framework constructed from divacant Keggin polyoxoanions and silver coordination compounds. Their structural differences indicate that the pH value of the reaction system plays a key role on the structures and topologies of these complexes, and the whole self-assembly process is pH-dependent.

Introduction

The rational design and synthesis of organic−inorganic hybrid materials based on the polyoxometalate (POM) inorganic building blocks and transition metal coordination compounds is still an appealing challenge.[1] As is well-known, the suitable combination of POM/metal/ligand is a main factor of design and construction of POM-based hybrids.[2] POMs, which are a large variety of oxygen-bridged metal clusters with unique structural characteristics and diversity of electronic structures, exhibit versatile applications in given fields, especially in catalysis, medicine, biology, electrochromism, magnetism, and material science.[1−3] POMs can act as unusually effective ligands to coordinate various transition metal ions because of their high electronic density.[4] Many complexes constructed from Keggin,[5] Wells−Dawson,[6] Anderson,[7] and Lindquist[8] type POM clusters and metal coordination compounds have been synthesized. On the other hand, Ag(I), as a d^{10} transition metal, possesses high affinity for N and O donors, flexible coordination number of

*To whom correspondence should be addressed. E-mail: rcao@fjirsm.ac.cn. Phone: + 86 591 83796710. Fax: + 8659183796710.

(1) (a) Hill, C. L.; Prosser-McCartha, C. M. *Coord. Chem. Rev.* **1995**, *143*, 407. (b) Mizuno, N.; Misono, M. *Chem. Rev.* **1998**, *98*, 199. (c) Rhule, J. T.; Hill, C. L.; Judd, D. A.; Schinazi, R. F. *Chem. Rev.* **1998**, *98*, 327. (d) Yamase, T. *Chem. Rev.* **1998**, *98*, 307. (e) Khenkin, A. M.; Weiner, L.; Wang, Y.; Neumann, R. *J. Am. Chem. Soc.* **2001**, *123*, 8531. (f) Kortz, U.; Mbomekalle, I. M.; Keita, B.; Nadjo, L.; Berthet, P. *Inorg. Chem.* **2002**, *41*, 6412. (g) Okun, N. M.; Anderson, T. M.; Hardcastle, K. I.; Hill, C. L. *Inorg. Chem.* **2003**, *42*, 6610. (h) Hill, C. L. *Angew. Chem., Int. Ed.* **2004**, *43*, 402.

(2) (a) Sha, J. Q.; Peng, J.; Zhang, Y.; Pang, H. J.; Tian, A. X.; Zhang, P. P.; Liu, H. *Cryst. Growth Des.* **2009**, *9*, 1708. (b) Pang, H. J.; Peng, J.; Sha, J. Q.; Tian, A. X.; Zhang, P. P.; Chen, Y.; Zhu, M. *J. Mol. Struct.* **2009**, *921*, 289.

(3) (a) Won, B. K.; Voitl, T.; Rodríguez-Rivera, G. J.; Dumesic, J. A. *Science* **2004**, *305*, 1280. (b) Mizuno, N.; Yamaguchi, K.; Kamata, K. *Coord. Chem. Rev.* **2005**, *249*, 1944. (c) Wei, M.; He, C.; Hua, M.; Duan, C. Y.; Li, S.; Meng, Q. J. *J. Am. Chem. Soc.* **2006**, *128*, 13318. (d) Zhao, J. W.; Zhang, J.; Zheng, S. T.; Yang, G. Y. *Inorg. Chem.* **2007**, *46*, 10944. (e) Hussain, F.; Bassil, B. S.; Kortz, U.; Kholdeeva, O. A.; Timofeeva, M. N.; Olivera, P.; Keita, B.; Nadjo, L. *Chem.—Eur. J.* **2007**, *13*, 4733. (f) Nsouli, N. H.; Bassil, S. B.; Dickman, M. H.; Kortz, U.; Keita, B.; Nadjo, L. *Inorg. Chem.* **2006**, *45*, 3858. (g) Pichon, C.; Mialane, P.; Dolbecq, A.; Marrot, J.; Riviére, E. R.; Bassil, B. S.; Kortz, U.; Keita, B.; Nadjo, L.; Sécheresse, F. *Inorg. Chem.* **2008**, *47*, 11120. (h) Zhu, Y. L.; Wang, L. S.; Hao, J.; Yin, P. C.; Zhang, J.; Li, Q.; Zhu, L.; Wei, Y. G. *Chem.—Eur. J.* **2009**, *15*, 3076.

(4) (a) Hagrman, P. J.; Hagrman, D.; Zubieta, J. *Angew. Chem., Int. Ed.* **1999**, *38*, 2638. (b) Yang, W. B.; Lu, C. Z.; Zhuang, H. H. *J. Chem. Soc., Dalton Trans.* **2002**, 2879.

(5) (a) Yokoyama, A.; Kojima, T.; Ohkubo, K.; Fukuzumi, S. *Chem. Commun.* **2007**, 3997. (b) Wang, J. P.; Zhao, J. W.; Duan, X. Y.; Niu, J. Y. *Cryst. Growth Des.* **2006**, *6*, 507. (c) Liu, C. M.; Zhang, D. Q.; Zhu, D. B. *Cryst. Growth Des.* **2006**, *6*, 524. (d) Uehara, K.; Nakao, H.; Kawamoto, R.; Hikichi, S.; Mizuno, N. *Inorg. Chem.* **2006**, *45*, 9448. (e) Sha, J. Q.; Peng, J.; Tian, A. X.; Liu, H. S.; Chen, J. *Cryst. Growth Des.* **2007**, *7*, 2535. (f) Ren, Y. P.; Kong, X. J.; Long, L. S.; Huang, R. B.; Zheng, L. S. *Cryst. Growth Des.* **2006**, *6*, 572. (g) Sun, Y. H.; Cui, X. B.; Xu, J. Q.; Ye, L.; Li, Y.; Lu, J. *J. Solid State Chem.* **2001**, *159*, 209. (h) Fan, L. L.; Xiao, D. R.; Wang, E. B.; Li, Y. G.; Su, Z. M.; Wang, X. L.; Liu, J. *Cryst. Growth Des.* **2007**, *7*, 592.

Published on Web 12/21/2009

two to seven in covalent complexes, and versatile geometries, such as "linear", "seesaw", "square pyramidal", and "trigonal bipyramidal" coordination geometries, and so forth.[2b,6a,9] These features make Ag(I) often be used as a metallic linker and a good candidate in constructing metal-organic frameworks. Moreover, ligands also play a key role in the formation of complexes owing to their different steric effect, soft-rigid degree, and structure.[10] The 2,2′-bipyridine and 1,10-phenanthroline are prone to form isolated low dimensional complexes, while the 4,4′-bipyridine is prone to form infinite structures exhibiting high dimensions.[11] Recently, we have reported a series of POM hybrids with 2, 2′-bipyridine and 1,10-phenanthroline ligand exhibiting one-dimensional (1D) or two-dimensional (2D) structures.[12] This inspired us to use other ligands, such as 4,4′-bipyridine, to synthesize a high dimensional hybrid and to study the effect on the structural dimension.

Some other factors, such as pH value, initial reactant, starting concentration, and reaction temperature, can influence the outcome of reaction in the construction of POM-based organic−inorganic hybrid materials under hydrothermal condition.[13] Many researchers have made efforts to understand fully the influence factors. Peng's group reported two high-dimensional and high-connected silver complexes of POMs by using the pre-synthesized Wells−Dawson POM building blocks at different pH values.[6a] Long's group have also studied the influences of the pH values on the structures of complexes based on pre-synthesized Keggin POMs.[13a] However, the research on how to control the initial pH value of the system to synthesize *in situ* organic−inorganic hybrids based on Keggin or Wells−Dawson type POM building blocks and silver coordination compounds with 4,4′-bpy ligands has been not reported yet.

Herein, we will report four organic−inorganic hybrids based on Keggin or Wells−Dawson POMs and silver coordination compounds with 4,4′-bipyridine ligand, formulated as, $[Ag_2(4,4'\text{-bpy})_2(4,4'\text{-Hbpy})(H_2O)][PW_{12}O_{40}]$ (4,4′-bpy = 4,4′-bipyridine, **1**), $[Ag_4(4,4'\text{-bpy})_4][4,4'\text{-}H_2bpy][P_2W_{18}O_{62}]\cdot 4H_2O$ (**2**), $[Ag_4(4,4'\text{-bpy})_4][H_2P_2W_{18}O_{62}]\cdot 7H_2O$ (**3**), and $Na_8[Ag_3(4,4'\text{-bpy})_3][PW_{10}Ag_2O_{39}]\cdot 6H_2O$ (**4**), which were hydrothermally synthesized *in situ* via adjusting the pH value of the system under similar conditions.

Experimental Section

Materials and Measurements. All chemicals were commercially purchased and used without purification. The hydrothermal reactions were carried out in 25 mL Teflon-lined stainless steel autoclaves under autogenous pressure with a fill factor of approximately 70%. Elemental analyses (C, H, and N) were carried on an Elementar Vario EL III analyzer. Cu, W, and P were determined by a Jobin Yvon Ultima2 ICP atomic emission Spectrometer. Infrared (IR) spectra were recorded in the range 400−4000 cm^{-1} on a Perkin-Elmer Spectrum using KBr pellets. Thermogravimetric analysis was recorded with a NETZSCH STA449C unit at a heating rate of 10 °C min^{-1} under nitrogen atmosphere.

Synthesis of $[Ag_2(4,4'\text{-bpy})_2(4,4'\text{-Hbpy})(H_2O)][PW_{12}O_{40}]$ (1). A mixture of $Na_2WO_4\cdot 2H_2O$ (0.408 g, 1.24 mmol), H_3PO_4 (0.5 mL, 85%), $AgNO_3$ (0.067 g, 0.39 mmol), 4,4′-bipyridine (0.043 g, 0.22 mmol), and H_2O (18 mL) was stirred for 30 min or so, and the pH value was adjusted to about 0−1 with 2 M NaOH. Finally, the resulting suspension was transferred to a Teflon-lined autoclave (25 mL) and kept at 160 °C for 5 days. After slow cooling to room temperature for 2 days, yellow needle crystals of **1** (yield about 33% based on Ag) were obtained by filtration, washed with distilled water and dried in desiccators at ambient temperature. Anal. Calcd for $C_{30}H_{27}Ag_2N_6O_{41}PW_{12}$ (3580.49): C, 10.06%; H, 0.76%; N, 2.35%; Ag, 6.03%; P, 0.87%; W, 61.61%. Found: C, 9.89%; H, 0.71%; N, 2.30%; Ag, 6.12%; P, 0.90%; W, 61.76%.

Synthesis of $[Ag(4,4'\text{-bpy})]_4[4,4'\text{-}H_2bpy][P_2W_{18}O_{62}]\cdot 4H_2O$ (2). Complex **2** was prepared similar to **1**, except that the pH value of the system was adjusted to about 1.5−2 with 2 M NaOH solution. Yellow sheet crystals suitable for X-ray analyses were obtained in about 31% yield based on Ag. Anal. Calcd for $C_{50}H_{50}Ag_4N_{10}O_{66}P_2W_{18}$ (5649.72): C, 10.63%; H, 0.89%; N, 2.48%; Ag, 7.64%; P, 1.10%; W, 58.57%. Found: C, 10.51%; H, 0.81%; N, 2.39%; Ag, 7.72%; P, 1.17%; W, 58.73%.

Synthesis of $[Ag_4(4,4'\text{-bpy})_4][H_2P_2W_{18}O_{62}]\cdot 7H_2O$ (3). Complex **3** was prepared similar to **1**, except that the pH value of the system was adjusted to about 3−3.5 with 2 M NaOH solution. Yellow prism crystals suitable for X-ray analyses were obtained in about 35% yield based on Ag. Anal. Calcd for $C_{40}H_{44}Ag_4N_8O_{67}P_2W_{18}$ (5527.02): C, 8.69%; H, 0.80%; N, 2.03%; Ag, 7.81%; P, 1.12%; W, 59.87%. Found: C, 8.57%; H, 0.72%; N, 1.97%; Ag, 7.96%; P, 1.20%; W, 60.01%.

Synthesis of $Na_8[Ag_3(4,4'\text{-bpy})_3][PW_{10}Ag_2O_{39}]\cdot 6H_2O$ (4). Complex **4** was prepared similar to **1**, except that the pH value of the system was adjusted to about 5.5−6 with 2 M NaOH solution. Colorless prism crystals suitable for X-ray analyses were obtained in about 29% yield based on Ag. Anal. Calcd for $C_{30}H_{36}Ag_5N_6Na_8O_{45}PW_{10}$ (3793.39): C, 9.50%; H, 0.96%; N, 2.22%; Na, 4.85; Ag, 14.22%; P, 0.82%; W, 48.46%. Found: C, 9.39%; H, 0.90%; N, 2.12%; Na, 4.71; Ag, 14.31%; P, 0.89%; W, 48.62%.

(6) (a) Sha, J. Q.; Peng, J.; Lan, Y. Q.; Su, Z. M.; Pang, H. J.; Tian, A. X.; Zhang, P. P.; Zhu, M. *Inorg. Chem.* **2008**, *47*, 5145. (b) Yan, B. B.; Xu, Y.; Bu, X. H.; Goh, N. K.; Chia, L. S.; Stucky, G. D. *J. Chem. Soc., Dalton Trans.* **2001**, 2009. (c) Niu, J. Y.; Guo, D. J.; Wang, J. P.; Zhao, J. W. *Cryst. Growth Des.* **2004**, *4*, 241. (d) Laronze, N.; Marrot, J.; Hervé, G. *Chem. Commun.* **2003**, 2360. (e) Yang, H. X.; Lin, J. X.; Chen, J. T.; Zhu, X. D.; Gao, S. Y.; Cao, R. *Cryst. Growth Des.* **2008**, *8*, 2623. (f) Tian, A. X.; Ying, J.; Peng, J.; Sha, J. Q.; Han, Z.; Ma, J. F.; Su, Z. M.; Hu, N.; Jia, H. *Inorg. Chem.* **2008**, *47*, 3274. (g) Lin, B. Z.; He, L. W.; Xu, B. H.; Li, X. L.; Li, Z.; Liu, P. D. *Cryst. Growth Des.* **2009**, *9*, 273.

(7) (a) Mankkumari, S.; Shivaiah, V.; Das, S. K. *Inorg. Chem.* **2002**, *41*, 6953. (b) Zhou, D. P.; Yang, D. *Acta Crystallogr.* **2007**, *E63*, i113. (c) An, H. Y.; Li, Y. G.; Wang, E. B.; Xiao, D. R.; Sun, C. Y.; Xu, L. *Inorg. Chem.* **2005**, *44*, 6062.

(8) (a) Anderson, T. M.; Thoma, S. G.; Bonhomme, F.; Rodriguez, M. A.; Park, H.; Parise, J. B.; Alam, T. M.; Larentzos, J. P.; Nyman, M. *Cryst. Growth Des.* **2007**, *7*, 719.

(9) (a) Nogueira, H. I. S.; Paz, F. A. A.; Teixeira, P. A. F.; Klinowski, J. *Chem. Commun.* **2006**, 2953.

(10) (a) Ren, Y. P.; Kong, X. J.; Hu, X. Y.; Sun, M.; Long, L. S.; Huang, R. B.; Zheng, L. S. *Inorg. Chem.* **2006**, *45*, 4016. (b) Venkatakrishnan, T. S.; Rajamani, R.; Ramasesha, S.; Sutter, J. P. *Inorg. Chem.* **2007**, *46*, 9569. (c) Chen, J.; Sha, J. Q.; Peng, J.; Shi, Z. Y.; Tian, A. X.; Zhang, P. P. *J. Mol. Struct.* **2009**, *917*, 10. (d) Tian, A. X.; Ying, J.; Peng, J.; Sha, J. Q.; Pang, H. J.; Zhang, P. P.; Chen, Y.; Zhu, M.; Su, Z. M. *Cryst. Growth Des.* **2008**, *8*, 3717. (e) Jin, H.; Qi, Y. F.; Wang, E. B.; Li, Y. G.; Wang, X. L.; Qin, C.; Chang, S. *Cryst. Growth Des.* **2006**, *6*, 2693.

(11) (a) Luan, G. Y.; Li, Y. G.; Wang, S. T.; Wang, E. B. *J. Chem. Soc., Dalton Trans.* **2003**, 233. (b) Sha, J. Q.; Peng, J.; Chen, J.; Liu, H. S.; Chen, J.; Dong, B. X.; Tian, A. X.; Su, Z. M. *Eur. J. Inorg. Chem.* **2007**, *126*, 1268.

(12) Yang, H. X.; Guo, S. P.; Tao, J.; Lin, J. X.; Cao, R. *Cryst. Growth Des.* **2009**, *9*, 4735.

(13) (a) Zheng, P. Q.; Ren, Y. P.; Long, L. S.; Huang, R. B.; Zheng, L. S. *Inorg. Chem.* **2005**, *44*, 1190. (b) Wang, J. P.; Ma, P. T.; Zhao, J. W.; Niu, J. Y. *Inorg. Chem. Commun.* **2007**, *10*, 523. (c) Soghomonian, V.; Chen, Q.; Haushalter, R. C.; Zubieta, J.; O'Connor, J. C. J.; Leelc, Y. S. *Chem. Mater.* **1993**, *5*, 1690. (d) LaDuca, R. L.; Rarig, R. S.; Zubieta, J. *Inorg. Chem.* **2001**, *40*, 607. (e) Hagrman, P. J.; Zubieta, J. *Inorg. Chem.* **2001**, *40*, 2800. (f) Pamela, Z. J.; Robert, L. J.; Randy, S. R., Jr.; Kenneth, M. J.; Zubieta, J. *Inorg. Chem.* **1998**, *37*, 3411. (g) Zhao, J. W.; Jia, H. P.; Zhang, J.; Zheng, S. T.; Yang, G. Y. *Chem.—Eur. J.* **2007**, *13*, 10030. (h) Chen, S. M.; Lu, C. Z.; Zhang, Q. Z.; Liu, J. H.; Wu, X. Y. *Eur. J. Inorg. Chem.* **2005**, 423.

Table 1. Crystal Data and Structure Refinements for Complexes **1**−**4**

	1	**2**	**3**	**4**
empirical formula	$C_{30}H_{27}Ag_2N_6O_{41}PW_{12}$	$C_{50}H_{50}Ag_4N_{10}O_{66}P_2W_{18}$	$C_{40}H_{48}Ag_4N_8O_{70}P_2W_{18}$	$C_{30}H_{36}Ag_5N_6Na_8O_{45}PW_{10}$
Fw	3580.49	5649.72	5563.57	3793.39
crystal system	monoclinic	orthorhombic	monoclinic	monoclinic
space group	*P*2(1)/*c*	*Pbcn*	*P*2(1)/*c*	*P*2/*c*
a (Å)	11.934(4)	24.789(5)	15.518(8)	16.85(2)
b (Å)	23.136(8)	22.241(5)	17.844(8)	11.236(15)
c (Å)	11.076(4)	17.334(4)	35.101(17)	22.86(2)
α (deg)	90	90	90	90
β (deg)	109.931(6)	90	96.001(7)	125.46(7)
γ (deg)	90	90	90	90
volume (Å^3)	2875.1(16)	9557(4)	9666(8)	3525(7)
Z	2	4	4	2
D_c/mg cm^{-3}	4.136	3.927	3.787	3.586
total reflns	21625	71318	71887	22642
unique reflns	6468	10962	22034	8013
R(int)/*R*(*σ*)	0.0773/0.0564	0.0873/0.0475	0.0993/0.0736	0.0898/0.0713
GOF	1.115	1.113	1.096	1.066
final *R* indices [$I < 2\sigma(I)$]	$R_1{}^a = 0.0451$	$R_1{}^a = 0.0547$	$R_1{}^a = 0.0798$	$R_1{}^a = 0.0695$
	$wR_2{}^b = 0.1151$	$wR_2{}^b = 0.1393$	$wR_2{}^b = 0.1676$	$wR_2{}^b = 0.1258$
indices (all data)	$R_1{}^a = 0.0562$	$R_1{}^a = 0.0647$	$R_1{}^a = 0.0961$	$R_1{}^a = 0.0756$
	$wR_2{}^b = 0.1330$	$wR_2{}^b = 0.1466$	$wR_2{}^b = 0.1863$	$wR_2{}^b = 0.1532$

$^a R_1 = \sum||F_o| - |F_c||/\sum|F_o|$. $^b wR_2 = \{\sum w(F_o{}^2 - F_c{}^2)^2/\sum w(F_o{}^2)^2\}^{1/2}$.

X-ray Crystallography. Structural measurements for complexes **1**−**4** were performed on a Mercury CCD (2 × 2 bin mode) diffractometer with graphite monochromated Mo Kα radiation ($\lambda = 0.71073$ Å) at 20 °C. Empirical from equivalents were made from *ψ*-scan data using the program SHELXTL 97 at the data reduction stage along with the correction for Lorentz and polarization effects.[14] The structure analysis was performed by using the Crystal Structure crystallographic program package. The structures of complexes **1**−**4** were solved by the direct methods (Wingx32, SIR-92), and successive Fourier difference syntheses. The final structures were examined with the program PLATON and no additional symmetry element was detected.[15] In complex **1**, the N3 and the water molecule (O1w) alternately coordinated with Ag^+, and another one nitrogen atom (N4) was protonated for the requirement of charge balance. So the 4,4′-bpy ligand including N3 and N4, and the water molecule are disordered. The bond lengths and bond angles of the disordered atoms are restrained in the range of usual values. For complex **3**, the noncoordinate waters, (O1w, O2w, O3w, O4w, O5w, O7w, O8w, O9w, O10w, and O2w′), are disordered according to a Fourier difference map by re-refinement, and the occupancy factors of them are not 100%. There are seven waters molecules in the unit cell, which is in agreement with thermogravimetry (TG) analyses. In complex **4**, the oxygen atoms (O10, O10, O15, O15′, O17, O17′, O18, and O18′) are also disordered, and each of them occupies 0.5. All the heavy atoms of complexes **1**−**4** were refined with anisotropic thermal parameters. These data can be obtained free of charge at the Cambridge Crystallographic Data Centre (CCDC, www.ccdc.cam.ac.uk/conts/retrieving.html). Crystal parameters and other experimental details of the data collection for complexes **1**−**4** are summarized in Table 1. Selected bond lengths and bond angles are listed in Supporting Information, Tables S1−S4. The CCDC reference numbers are 733468−733471 for complexes **1**−**4**, respectively.

Results and discussion

Syntheses. Complexes **1**−**4** reported here were synthesized under traditional hydrothermal methods, which have now been demonstrated as effective in the synthesis of organic−inorganic hybrid materials of POMs. With the aim of studying the influence of the pH value on the final products, the self-assembly reactions of $Na_2WO_4 \cdot 2H_2O$, H_3PO_4, $AgNO_3$, 4,4′-bipyridine, and H_2O were carried out at different pH value under similar condition. As expected, four different structural complexes exhibiting high dimensional frameworks were successfully synthesized, which shows that the pH value plays a key role during the formation of complexes. The formations of complexes **1**−**4** are shown in Scheme 1.

Scheme 1. Schematic Illustration of the Synthesis Routes of Complexes **1**−**4**

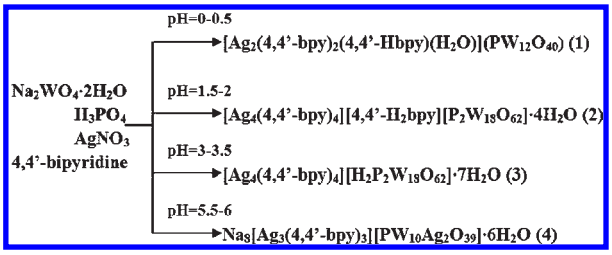

Crystal structures. The W−O and P−O bond lengths of complexes **1**−**4** are in the normal ranges (Supporting Information, Tables S1−S4). Bond valence sum calculations[16] show that all tungsten atoms are in +6 oxidation states, and all silver atoms are in +1 oxidation state in complexes **1**−**3**. In complex **4**, all sodium and silver atoms are in +1 oxidation state, and all tungsten atoms are in +6 oxidation state.

Complex **1** was obtained at a very low pH value about 0−0.5 under hydrothermal condition. Single-crystal X-ray diffraction analysis reveals that complex **1** consists of a Keggin polyoxoanion $[PW_{12}O_{40}]^{3-}$, two silver ions, three 4,4′-bpy ligands, and one coordination water (Figure 1a). The Keggin cluster in **1** is the classical saturated α-Keggin cluster consisting of four groups of trimetallic $(WO_6)_3$ units. Each WO_6 octahedron in a trimetallic unit shares an edge with a neighboring one,

(14) Sheldrick, G. M. *SHELXTL 97, A program for the refinement of crystal structures*; University of Göttingen: Göttingen, Germany, 1997.

(15) Spek, A. L. *PLATON, A multipurpose crystallographic tool*; Utrecht University: Utrecht, The Netherlands, 1999.

(16) Brown, I. D.; Altermatt, D. *Acta Crystallogr.* **1985**, *B41*, 244.

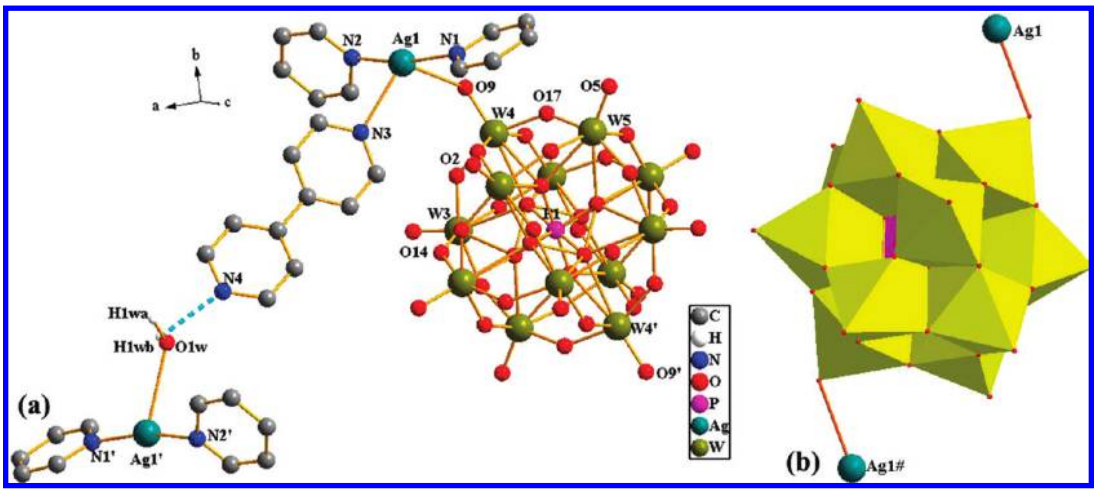

Figure 1. (a) Structure of complex **1**. (b) View of coordination details of Keggin type POM polyoxoanion of complex **1** (#1, 2−*x*, 2−*y*, 2−*z*).

and the $(WO_6)_3$ units link together via corner sharing WO_6 octahedra to form a cluster cage with a PO_4 tetrahedron located in the center. The Keggin cluster can be viewed as bidentate inorganic ligand to coordination with two silver atoms via Ag−O weak interaction (Ag1−O9 = 2.858 Å) (Figure 1b).

The most important feature of complex **1** is that it contains an interesting 3-fold interpenetration of diamondlike network in POM hybrid materials. To illustrate the interpenetration topology in complex **1**, we shall first omit the POM building blocks. It should be noted that the disordered coordination water (O1w) can interact with N4 of the disordered 4,4′-bpy ligand via hydrogen bonding (O1w−N4 2.76 Å, Supporting Information, Table S1). It is very interesting that the Ag1 ions coordinate to the nitrogen atoms (N1, N2) of 4,4′-bpy ligands to form a remarkably long rod (Ag1−N1 = 2.171(10) Å, Ag1−N2 = 2.171(10) Å, see Table 2). The Ag---Ag---Ag angle is 172.46° and the adjacent Ag distance is 10.65 Å. These long rods are linked by the disordered O(1w) and the disordered 4,4′-bpy via hydrogen bonding (O1w−H1wb---N4), Ag−N coordination interaction (Ag1−N3), and Ag−O weak interaction (Ag1---O1w). Thus, a (6, 3)-topological coordination layer was formed along the *ab* plane, if the Ag atoms are considered as nodes (Supporting Information, Figure S1). While the saturated Keggin polyoxoanions act as bidentate ligands to link the layers to a three-dimensional (3D) network via the Ag−O weak interaction. So each Ag is 4-connection and has four 6-membered windows (Figure 2a). Each network is composed of tetrahedral Ag atoms bridged by 2-connection POM building blocks and 4,4′-bpy ligands. Schematic presentation of a single 3D network of **1** was shown in Figure 2b. And the entire structure can be described as an extended framework constructed from $[Ag_2(4,4'\text{-bpy})_2(Hbpy)(H_2O)]^{3+}$ cations attached by polyoxoanion cluster linkages. As shown in Figure 2c, complex **1** contains an interesting 3-fold interpenetration of diamondlike network via coordination bond, Ag---O weak interaction, and hydrogen bonding.

In contrast to the Keggin polyoxoanion in complex **1**, complex **2** consists of one Wells−Dawson type polyoxoanion $[P_2W_{18}O_{62}]^{6-}$, four $[Ag(4,4'\text{-bpy})]^+$ cations, one protonated 4,4′-bpy molecule, and four noncoordinated water molecules (Figure 3a). One interesting structural feature of complex **2** is that the Wells−Dawson unit acts as an octa-dentate ligand toward Ag^+ through eight terminal oxygens located at the "cap" or "belt" site (Figure 3b). To our knowledge, complex **2** represents the highest coordination number of Wells−Dawson polyoxoanions at present, which helps to lead the formation of high-connected Wells−Dawson POMs. Another structural feature is that the two crystallographically independent silver atoms show the same coordination geometries in the structure. Both Ag1 and Ag2 exhibit a four-coordinated "seesaw" geometry of $\{AgN_2O_2\}$ formed by two N atoms from the 4,4′-bpy ligand and two O atoms located at the "belt" and "cap" site of two Dawson type POMs, which are terminal oxygen atoms of POMs.

Table 2. Selected Bond Lengths (Å) of Complexes **1**−**4**[a]

Complex 1					
Ag1−N1	2.172(10)	Ag1−O1w	2.886(10)	Ag1−O9	2.858(11)
Ag1−N2	2.203(12)	Ag1−N3	2.523(13)		
Complex 2					
Ag1−N2	2.151(4)	Ag1−O2	2.833(5)	Ag2−N4#1	2.162(3)
Ag1−N1	2.152(5)	Ag2−O2	2.705(5)	Ag2−N3	2.176(6)
Ag1−O1	2.637(4)	Ag2−O3	2.748(6)		
Complex 3					
Ag1−N2	2.20(2)	Ag3−N6	2.19(2)	Ag4−N7#4	2.12(3)
Ag1−N1	2.20 (18)	Ag3−N5	2.23(2)	Ag4−N8#5	2.14(2)
Ag1−O1	2.55(15)	Ag3−O2#2	2.72(15)	Ag4−O5	2.63(19)
Ag1−O2#1	2.72(18)	Ag3−O3#3	2.76(17)	Ag4−O4#6	2.73(2)
Ag2−N4	2.17(3)	Ag2−N3	2.20(4)		
Complex 4					
Ag1−N1	2.17(2)	Ag3−O2	1.97(3)	Ag4−O5	2.11(3)
Ag1−N1#2	2.17(2)	Ag3−O2#1	1.97(3)	Ag4−O5#1	2.11(3)
Ag1−O1	2.792	Ag3−O4	2.07(6)	Ag4−O19	2.53(5)
Ag1−O1#2	2.792	Ag3−O12#2	2.09(4)	Ag4−O4#3	1.93(6)
Ag2−N3	2.180(19)	Ag3−O12	2.09(4)	Ag4−O6#1	2.07(3)
Ag2−N2	2.18(2)	Ag3−O20	2.59(4)	Ag4−O6	2.07(3)
Ag2−O7	2.771				
Ag2−O8	3.028				

[a] Symmetry transformations used to generate equivalent atoms: For complex **2**: #1: −*x*+1/2, *y*−1/2, *z*. For complex **3**: #1: −*x*,*y*−1/2,−*z*+1/2; #2: −*x*+1, −*y*, −*z*+1; #3: *x*+1, −*y*−1/2, *z*+1/2 ; #4: *x*−1, *y*, *z*−1: #5: *x*+1, *y*, *z*; #6: −*x*+1, −*y*, −*z*. For complex **4**: #1: −*x*−1, *y*, −*z*−3/2; #2: −*x*, −*y*−1, −*z*; #3: *x*, *y*+1, *z*.

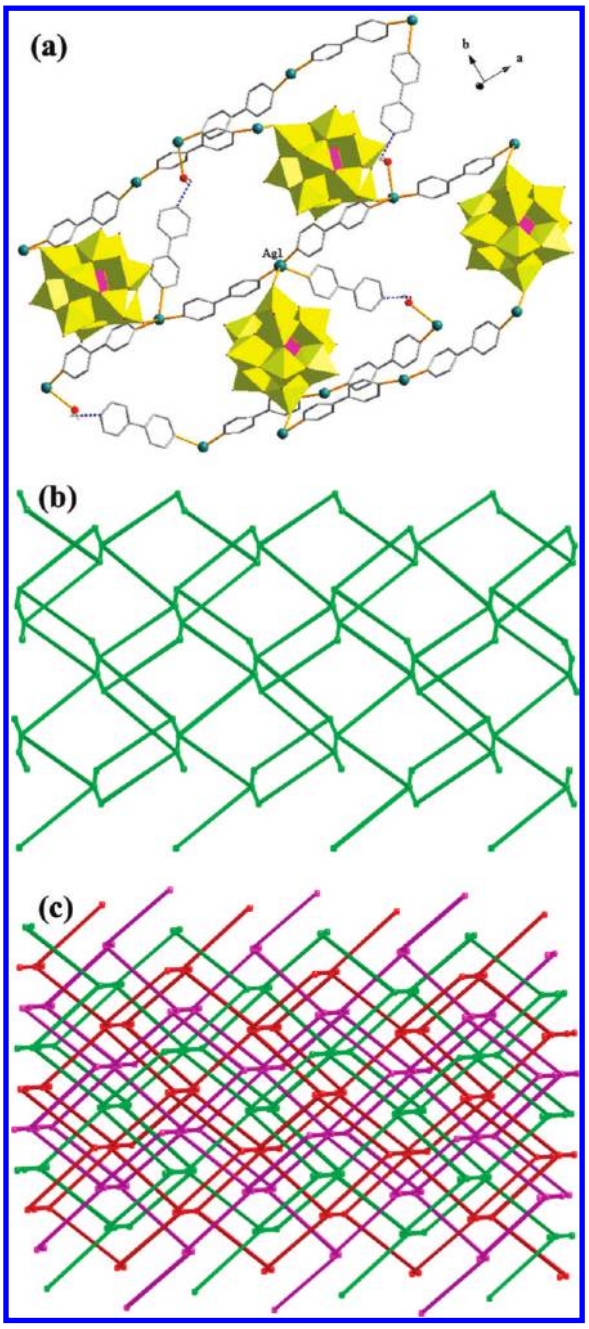

Figure 2. (a) View of the single net of complex **1**. (b) Schematic presentation of a single 3D network of **1**. (c) Interlocked units of 3-fold interpenetration diamondlike nets of complex **1**.

The bond distances around the Ag ions are 2.15−2.17 Å (Ag−N) and 2.63−2.83 Å (Ag−O), while the N−Ag−N angles are 164.9−175.9° and O−Ag−O angles are 148.7−152.6°.

The most striking structural feature of complex **2** is that the Ag(I) ions connect the Wells−Dawson POM building blocks to form a 2D network via Ag−O direct interaction along the *ac* plane (Figure 4a), which exhibits a (4,4) topology. In the 2D layer, each Ag atom links two adjacent Wells−Dawson polyoxoanions clusters, and each Wells−Dawson polyoxoanion provides eight terminal oxygen atoms linking with eight Ag atoms. While the spacer ligand 4,4′-bpy, which is prone to form infinite polymerized structures, directly coordinates silver to form an array of infinite $[Ag(4,4'\text{-bpy})]_n^{n+}$ chains along the *bc* plane (Figure 4b). Thus, the $[Ag(4,4'\text{-bpy})]_n^{n+}$ chains connect the 2D (4,4) topology network to further form a 3D framework, as shown in Figure 5a. Topological analysis of the complex **2** reveals a 2-nodal 4, 8-connected network with point symbol $(4\cdot6^4\cdot8)_4$-$(4^4\cdot6^{16}\cdot8^8)$ (Ag1 and Ag2 4-c nodes; $P_2W_{18}O_{62}$, 8-c node), which is new in binodal nets (Figure 5b).

The structure of the 3D Wells−Dawson phosphotungstate **3**, synthesized under conditions close to **1** and **2**, with the increase of pH value between 3 and 3.5, is much more complicated. Single crystal X-ray analysis shows that complex **3** crystallizes in the $P2_1/c$ space group, and consists of one Wells−Dawson polyoxoanion $[H_2P_2W_{18}O_{62}]^{6-}$, four $[Ag(4,4'\text{-bpy})]^+$ cations, and seven noncoordination water molecules (Figure 6a). The Wells−Dawson type polyoxoanion acts as hexa-dentate inorganic ligand toward Ag(I) ions (Figure 6b). Charge balance requires the presence of two free protons per formula unit, which were not located in the structure and may be associated with the Wells−Dawson cluster anion.[13b] The four crystallographically independent silver atoms (Ag1, Ag2, Ag3, and Ag4) exhibit three sorts of coordination geometries in the structure. Ag1 and Ag4 exhibit identical environments with two nitrogen atoms from 4,4′-bpy molecules (Ag−N = 2.12(3)−2.20(2) Å) and two oxygen atoms located at the "belt" and "cap" site of two Dawson type POMs (Ag−O = 2.55−2.73 Å), which are a "seesaw" structure; Ag2 is coordinated by two nitrogen atom from the 4,4′-bpy ligand (Ag−N = 2.17(3)−2.20(4)Å) exhibiting a linear structure; Ag3 forms a tetrahedral geometry, coordinated by two nitrogen atoms of the 4,4′-bpy ligand (Ag−N = 2.19(2)−2.23(2)Å) and two terminal oxygen atoms from the Wells−Dawson type polyoxoanions (Ag−O, 2.72−2.76 Å). These Ag ions connect the Wells−Dawson polyoxoanions and 4,4′-bpy molecules into a 3D framework.

The 3D network of complex **3** can be also considered being constructed from two moieties. As shown in Figure 7a, one moiety is the 2D layer based on Wells−Dawson polyoxoanions and silver ions. The 2D layer exhibits a (6,3) topology structure, each Ag atom covalently links two adjacent Wells−Dawson polyoxoanions clusters, and each Wells−Dawson polyoxoanion provides six terminal oxygen atoms linking with six Ag atoms. The other moiety is an array of infinite $[Ag(4,4'\text{-bpy})]_n^{n+}$ chains, shown in Figure 7b. The two moieties are fused together via Ag−O bonds, resulting in a 3D framework (Figure 8a). Topological analysis of complex **3** reveals a 3-nodal 4,6-connected network with a new topology. The Point (Schläfli) symbol, $(4\cdot6^4\cdot7)(4\cdot6^4\cdot8)_2$-$(4^3\cdot6^8\cdot7^2\cdot8^2)$, is fairly complicated because of the number of nodes (Ag(1), Ag(2) and Ag(3), 4-c nodes; $P_2W_{18}O_{62}$, 6-c node) as well as the multiple interconnections between Ag nodes (Figure 8b).

It is very interesting that with increase of the pH value of the system to 5.5−6, another novel complex **4** was obtained. Complex **4** consists of an Ag(I)-substituted Keggin type $[PW_{10}Ag_2O_{39}]^{11-}$ polyoxoanion, three $[Ag(4,4'\text{-bpy})]^+$ units, eight Na^+ cations, and six coordinated water molecules (Figure 9a). The POM unit in complex **4** is a divacant Keggin $[PW_{10}O_{39}]^{13-}$ anion functionalized by two Ag(I) ions, instead of a saturated

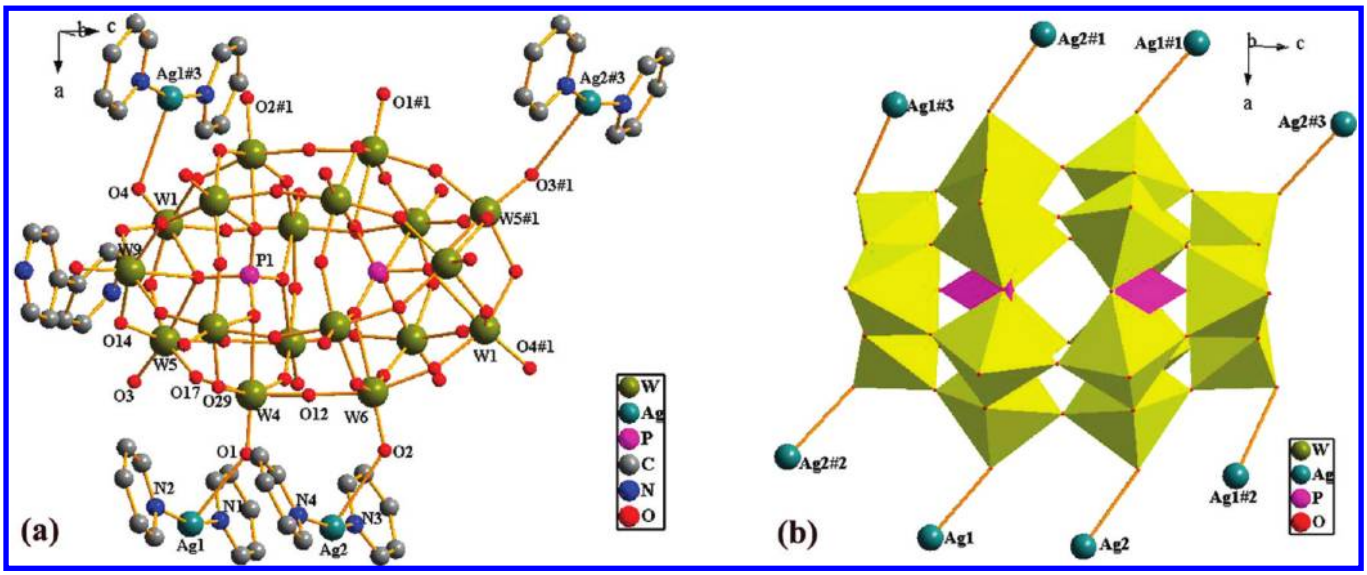

Figure 3. (a) Drawing of the asymmetric unit of complex **2**. The hydrogen atoms and solvent water molecules are omitted for clarity. (b) View of coordination details of Wells−Dawson type POM polyoxoanion of complex **2** (#1, $-x$, y, $-z+1/2$; #2, $0.5-x$, $0.5-y$, $0.5+z$; #3, $x-0.5$, $0.5-y$, $1-z$).

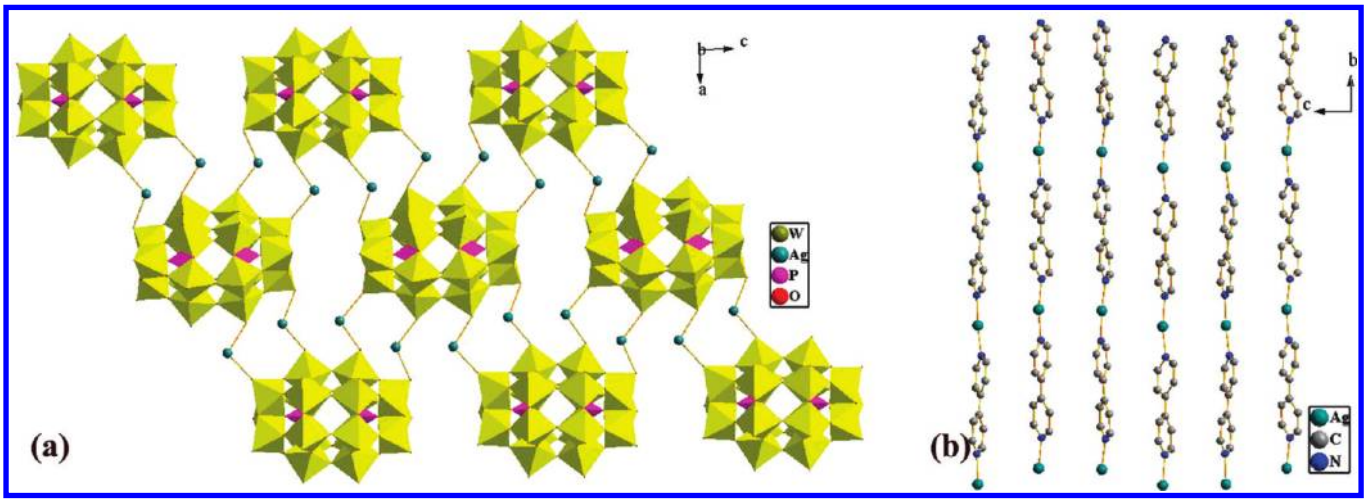

Figure 4. (a) View of the 2D network of complex **2** constructed by POMs and Ag ions. (b) Ball/Stick representation of $[Ag(4,4'\text{-bpy})]_n^{n+}$ chains of complex **2**.

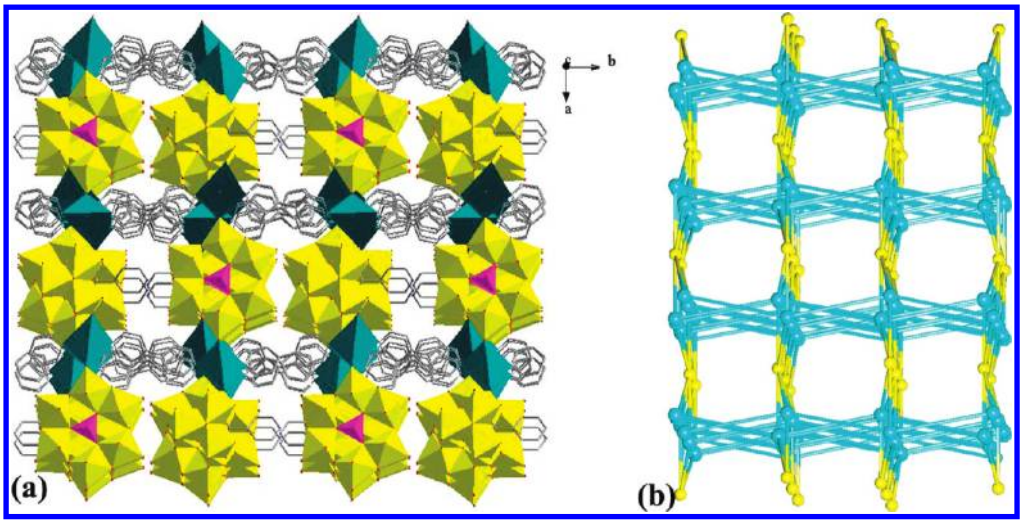

Figure 5. (a) View of 3D network in complex **2**. Yellow, teal, and pink polyhedrons show the $[WO_6]$, $[AgN_2O_x]$, and $[PO_4]$ units, respectively. (b) View of the topology of complex **2**.

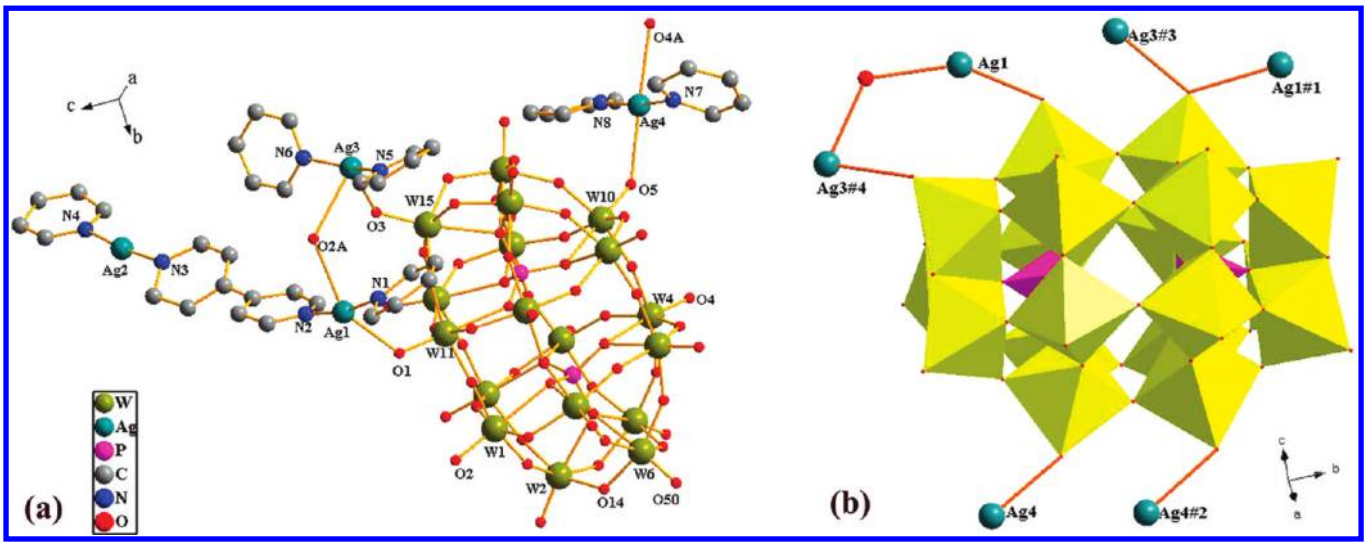

Figure 6. (a) Ball/stick representation of the molecular structure unit of **3**, $[Ag_4(4,4'\text{-bpy})_4][H_2P_2W_{18}O_{62}]\cdot 5H_2O$. (b) View of the coordinated details of the Wells−Dawson polyoxoanion in complex **3**. (#1, $-x$, $0.5+y$, $0.5-z$; #2, $1-x$, $-y$, $-z$; #3, $1-x$, $-y$, $1-z$; #4, $-1+x$, $-0.5-y$, $-0.5+z$.).

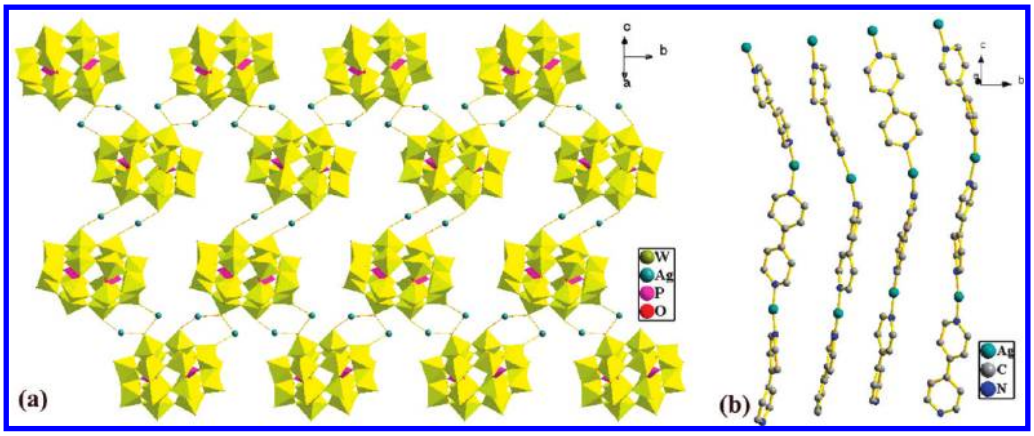

Figure 7. (a) View of the 2D network of complex **3** constructed by POMs and Ag ions. (b) Ball/Stick representation of $[Ag(4,4'\text{-bpy})]_n^{n+}$ chains of complex **3**.

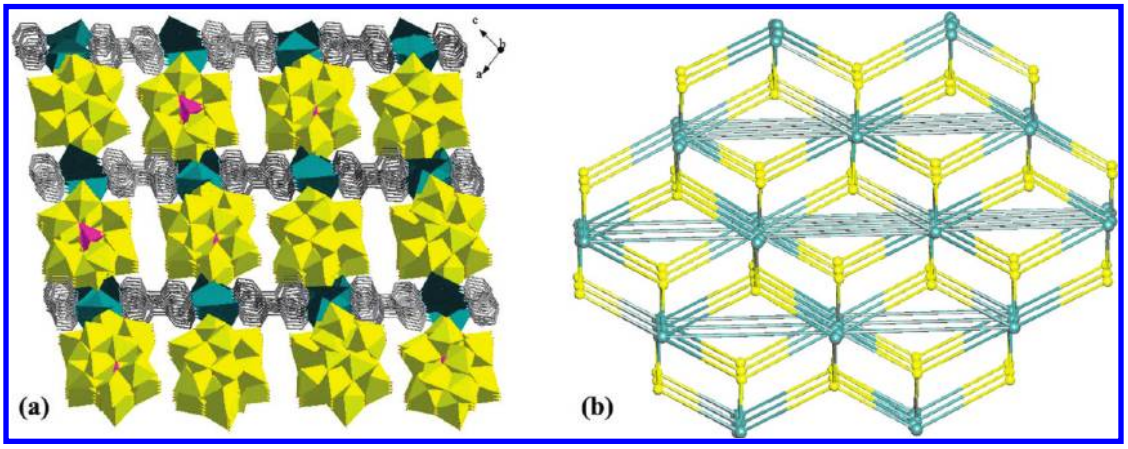

Figure 8. (a) View of 3D network in complex **3**. Yellow, teal, and pink polyhedrons show the $[WO_6]$, $[AgN_2O_x]$, and $[PO_4]$ units, respectively. (b) View of the topology of complex **3**. ($\{P_2W_{18}O_{62}\}$, yellow; $\{Ag_6\}$, gray blue).

POM, which is very different from the POM unit of complexes **1**−**3**. The divacant Keggin $[PW_{10}O_{39}]^{13-}$ anion acts as multidentate inorganic ligand toward 8 Ag(I) atoms and 12 Na(I) atoms, which is very rare in the POM-based hybrid. There are four crystallographically independent silver atoms (Ag1, Ag2, Ag3, Ag4), exhibiting three sorts of coordination geometries in the structure. Ag1 is coordinated by two nitrogen atoms from two 4,4′-bpy ligands (Ag−N = 2.17(2) Å), two terminal oxygen atoms (O1, O1′) of two divacant $[PW_{10}O_{39}]^{13-}$ polyoxoanions (Ag−O = 2.792 Å), exhibiting a plane geometry. Ag2 shows a trigonal geometry accomplished by two

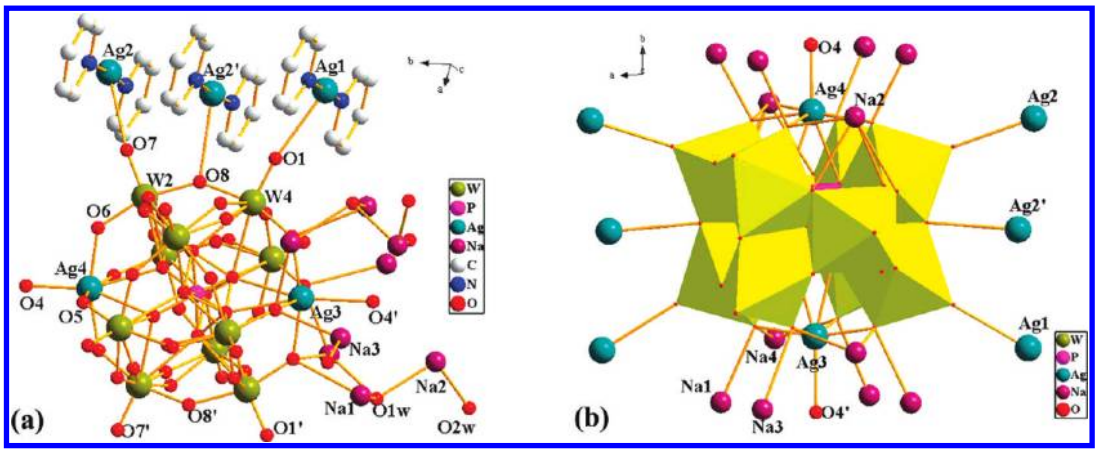

Figure 9. (a) Ball/stick representation of the molecular structure unit of **4**. (b) View of the coordinated details of the divacant $[PW_{10}O_{39}]^{13-}$ in complex **4**.

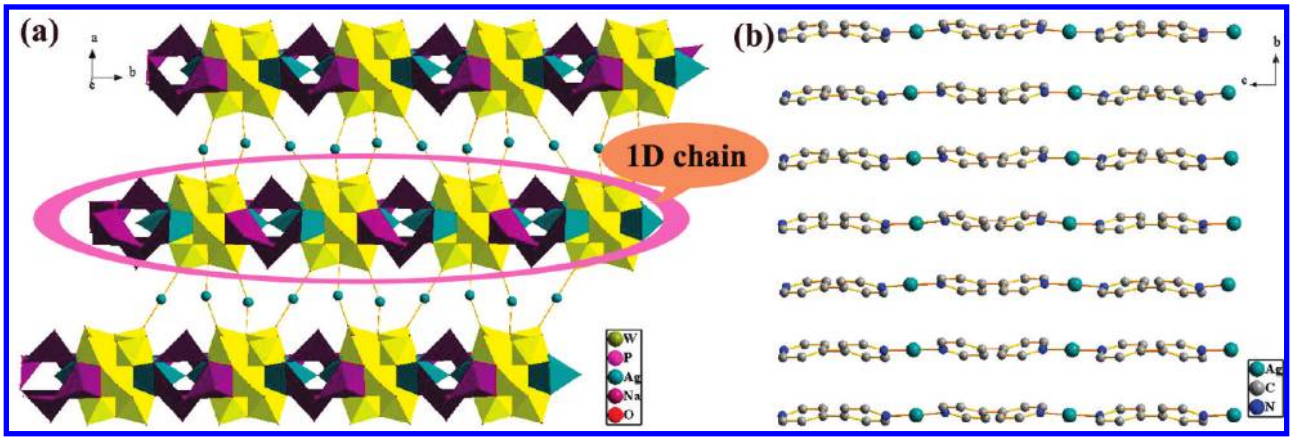

Figure 10. (a) View of the 2D network of complex **4** constructed by POMs and Ag ions. (b) Ball/Stick representation of $[Ag(4,4'\text{-bpy})]_n^{n+}$ chains of complex **4**.

nitrogen atoms of two 4,4′-bpy (Ag−N = 2.180(18) Å), one bridging oxygen atoms from the polyoxoanions (Ag2−O7 = 2.771 Å). The fourth potentially bonding position is occupied by O8 from the divacant Keggin anion with Ag2−O8 distance of 3.028(11) Å, which falls in the "Secondary Bonding" range and can considered as a weak coordination.[6a,17] Both Ag3 and Ag4 display similar coordination geometry of an octahedron sharing one apex O4, defined by six oxygen atoms of polyoxoanions (Ag−O distance, from 1.93(6) to 2.59(4) Å). Although the distance 1.93(6) Å is slightly short, it is longer than the Ag−O distance 1.842(9) Å reported in the literature.[16] It is noteworthy that O4 and the eight Na^+ ions (four crystallographically independent sodium atoms) connect the divacant Keggin polyoxoanions to form a 1D chain. The 1D chains are further linked by Ag1 and Ag2 to a 2D framework via Ag−O interaction, as shown in Figure 10a. Meanwhile, Ag1 and Ag2 atoms coordinate to 4,4′-bpy ligands to form an array of infinite $[Ag(4,4'\text{-bpy})]_n^{n+}$ chains along the *bc* plane (Figure 10b). Thus, the $[Ag(4,4'\text{-bpy})]_n^{n+}$ chains connect the 2D network to further form a 3D framework, as shown in Figure 11.

Influence of pH Value on the Structures of Complexes 1−4. Unambiguously, the different pH values play a key role on the formation of final products. When the same starting materials are selected, different POM complexes are hydrothermally synthesized at pH = 0−0.5 for **1**, 1.5−2 for **2**, 3−3.5 for **3**, and 5.5−6 for **4**, respectively, which indicates that the self-assembly process is pH-dependent. POM is very sensitive to H^+, and the pH

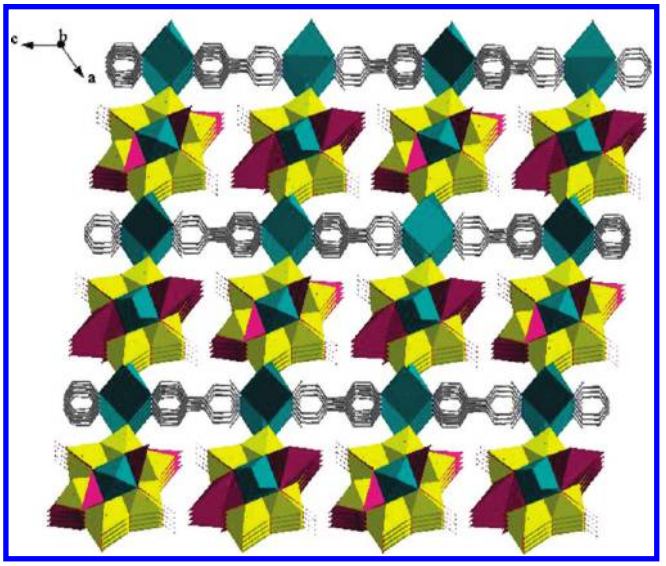

Figure 11. View of 3D network in complex **4**. Yellow, teal, and pink polyhedrons show the $[WO_6]$, $[AgN_2O_x]$, and $[PO_4]$ units, respectively.

(17) Huheey, J. E. *Inorganic Chemistry: Principles of Structure and Reactivity*, 2nd ed.; Harper & Row: New York, 1978.

value of the solution can influence the formation process of the final products.[18] The formation of different POM buliding blocks can be proposed as the following scheme (eqs 1−3). For the same concentration of precursors H_3PO_4 and Na_2WO_4 in aqueous solution, with the increase of pH value (namely, H^+ concentration is decreased), different type POM building blocks were obtained from the acidic solution (eqs 1−3).[18] In our experiment, at low pH, such as 0−1, the product is prone to form saturated Keggin POM building blocks. With the increase of pH to 1.5−3.5, Wells−Dawson POM in complexes **2**−**3** can be obtained. The difference of complexes **2** and **3** may be due to the ability of 4,4′-bpy of getting protons and the coordination ability of Wells−Dawson at different pH values. When the pH value is adjusted to 5.5−6, divacant Keggin POMs are formed. Thus, we can synthesize *in situ* different type POM-based organic−inorganic hybrids via adjusting the pH value of the reaction system.

$$PO_4^{3-} + 12WO_4^{2-} + 24H^+ \rightarrow [PW_{12}O_{40}]^{3-} + 12H_2O \quad (1)$$

$$PO_4^{3-} + 9WO_4^{2-} + 18H^+ \rightarrow 0.5[P_2W_{18}O_{62}]^{6-} + 9H_2O \quad (2)$$

$$PO_4^{3-} + 10WO_4^{2-} + 10H^+ \rightarrow [PW_{10}O_{39}]^{13-} + 5H_2O \quad (3)$$

IR Spectra, and TG Analyses. The infrared spectra of complexes **1**−**4** were recorded between 400 and 4000 cm^{-1} with KBr pellets (Supporting Information, Figure S2). The 1200−1700 cm^{-1} region is indicative of the 4,4′-bpy organic ligand. The P−O vibrations of complex **1** are observed only at 1079 cm^{-1}, which indicates that the polyoxoanion in **1** is the saturated $[PW_{12}O_{40}]^{3-}$ anion. The infrared spectra of complexes **2**−**3** are quite similar in the P−O region with one strong Wells−Dawson characteristic peak at 1091 cm^{-1}. While the P−O vibrations of **4** are split into two bands at 1041 and 1080 cm^{-1}, which confirms that in complex **4** the polyoxoanion is not the saturated $[PW_{12}O_{40}]^{3-}$ anion but, as suggested by the results of elemental and single crystal X-ray diffraction analyses, the superposition of a disubstituted Keggin anion.[19] The bands between 940 and 980 cm^{-1} are assigned to the $M{=}O_t$ (M = W) stretching vibrations, peaks between 700 and 900 cm^{-1} are attributed to $M-O_b-M$ stretching modes, and peaks between 550 and 700 cm^{-1} represent the $M-O_c-M$ vibrations.

The thermal stabilities of complexes **1**−**4** were investigated under N_2 atmosphere from 40 to 1000 °C, and the TG curves are provided in the Supporting Information, Figures S3−S7. The TG curve of **1** shows a multistep weight loss: the first weight loss of 0.59% (calcd 0.50%) before 240 °C corresponds to the loss of water, and the whole weight loss of 16.27% (calcd 15.58%) between 300 and 850 °C is attributable to the oxidation combustion of 4,4′-bipyridine organic groups and POM building blocks. The TG curves of **2**−**3** exhibit the first weight loss of 1.41% for **2** (calcd 1.27%) and 2.47% for **3** (calcd 2.27%) below 240 °C assigned to the removal of H_2O, and the whole weight loss of 18.72% for **2** (calcd 17.91%) and 17.44% for **3** (calcd 16.67%) at about 270−850 °C may be ascribed to the decomposition of organic ligands and POMs, respectively. For complex **4**, the first weight loss of 3.01% (calcd 2.85%) between 40 and 220 °C is assigned to the removal of H_2O, and the whole weight loss of 17.54% (calcd 16.81%) below 850 °C is attributed to the decomposition of organic ligands and POMs.

Conclusions

In summary, the successful design and construction of complexes **1**−**4** provides new examples of the utilities of Na_2WO_4 as raw material precursors and $AgNO_3$ as bridges in the presence of organic ligands for synthesizing *in situ* high-dimensional solid-state materials via adjusting the pH value of the system, which shows that the self-assembly process is pH-dependent. Complex **1**, based on saturated Keggin POM building block, exhibits an interesting 3-fold interpenetration of diamondlike network. Complexes **2**−**3**, constructed from Wells−Dawson polyoxoaninons and silver coordination compounds, reveal high-dimensional frameworks with new topologies $(4\cdot6^4\cdot8)_4(4^4\cdot6^{16}\cdot8^8)$ and $(4\cdot6^4\cdot7)(4\cdot6^4\cdot8)_2(4^3\cdot6^8\cdot7^2\cdot8^2)$, respectively. Different from complexes **1**−**3**, complex **4** forms a 3D framework consisting of divacant Keggin polyoxoanions and silver coordination compounds. This work may provide effective information for the construction of other high-dimensional network based on POM building blocks and transition metal coordination compounds.

Acknowledgment. This work was financially supported by 973 Program (2006CB932903, 2007CB815303), NSFC (20731005, 20821061, and 20873151), Fujian Key Laboratory of Nanomaterials (2006L2005) and Key project from CAS.

Supporting Information Available: X-ray crystallographic files for complexes **1**−**4** in CIF format and figures of some structures, IR spectra, and TG curves, and the tables with the bond distances and angles. This material is available free of charge via the Internet at http://pubs.acs.org.

(18) (a) Kytko, K. H.; Glemeser, O. *Adv. Inorg. Chem. Radiochem.* **1976**, *19*, 239. (b) Mbomekalle, I.; Lu, Y. W.; Keita, B.; Nadjo, L. *Inorg. Chem. Commun.* **2004**, *7*, 86. (c) Lan, Y. Q.; Li, S. L.; Wang, X. L.; Shao, K. Z.; Du, D. Y.; Zang, H. Y.; Su, Z. M. *Inorg. Chem.* **2008**, *47*, 8179. (d) Shishido, S.; Ozeki, T. *J. Am. Chem. Soc.* **2008**, *130*, 10588. (e) Graham, C. R.; Finke, R. G. *Inorg. Chem.* **2008**, *47*, 3679.

(19) Lisnard, L.; Dolbecq, A.; Mialane, P.; Marrot, J.; Codjovi, E.; Sécheresse, F. *Dalton Trans.* **2005**, 3913.